Laboratory experiments on the performance of an OWC-WEC: fixed condition versus floating platform-embodied condition

Lorenzo Cappietti, Irene Simonetti, Ilaria Crema

Abstract— **So far, Oscillating Water Column (OWC) devices have been proposed both for harvesting the wave energy and for attenuating the motion of floating platforms. In order to study the performance of the OWC device embodied in a Very Large Floating Structure (VLFS), a laboratory-scale physical model was manufactured and tested in the wave-current flume of LABIMA, the Laboratory of Maritime Engineering of University of Florence, Italy. Both regular and irregular waves were tested. The floating behaviour of the VLFS under the action of waves with different steepness was measured by using contactless ultrasonic distance sensors installed along the VLFS length. Moreover, the oscillation of the water level inside the OWC device, the differential pressure and the related air flow velocity through the duct hosing the power take off were measured. This work aims at describing the conducted laboratory experiments and to discuss the performance of the OWC devices integrated in the VLFS in terms of the comparison with the performance of the same OWC tested in fixed conditions. Under some specific design conditions, the platform-embodied OWC has a capture with ratio up to almost 3 times higher than the corresponding fixed device.**

Keywords—**Oscillating Water Column, Experimental modelling, Very Large Floating Platform, Capture width ratio.**

I. INTRODUCTION

The global interest toward renewable energies has been steadily increasing over the past years. The harvesting of Marine Renewable Energies (MRE) is an option and, to date, several Wave Energy Converters (WEC) have been proposed [1]. In this context, the Oscillating Water Column (OWC) is a well know concept for exploitation of the wave energy and it has been one of the first WECs to have reached the prototype scale with installation in the sea [2], [3].

In its basic form, an OWC is a hollow caisson, partially immersed below the sea surface, with an inner column of water and a volume of air above its free surface. A duct connects the internal air volume with the external atmosphere. The action of the external incident waves excites the internal water column that starts to oscillate and so the air volume above its free surface is alternatively compressed and decompressed.

This compression/decompression effect produces an oscillatory airflow through the duct. If a self-rectifying air turbine is placed in the duct, the oscillating air flow is transformed in a unidirectional rotational motion that activates a coaxial electrical generator [4].

The efficiency of the process in which wave-energy is transformed into pneumatic energy is called here after the primary efficiency (or capture width ratio) and its quantification is the objective of the present work. As for any other WEC based on oscillating masses, the maximization of the energy conversion efficiency is achieved if a resonant behaviour is triggered. It means that the natural frequency of the OWC, which is a function of its geometry, must be close to the characteristic frequency of the incident waves in the installation site.

The OWC is also counted in the literature as a possible device for attenuating the motion of Very Large Floating Structures (VLFSs) under the action of incident waves [5]. If on the one hand the OWCs modify the VLFS dynamic behaviour, on the other hand also the effectiveness of the OWC in harvesting the wave energy is altered with respect to the fixed condition. This work aims at investigating the differences in the wave energy harvestable with a fixed OWC and with the same device embodied into a VLFS.

The work here presented is an extension of two previous works [6, 7]. In [6], a first set of laboratory tests on an OWC device in fixed conditions were presented, finding a maximum value of the capture width ratio of the device in regular waves of 70%. Moreover, such value was later increased to 87% by means of a geometry optimization performed with numerical modelling, as documented in [8]. Wort to mention that these capture widths were achieved under the wave conditions that characterize Sea sites in front of the Tuscany coast, Italy. In [7], the effect of OWC devices in reducing the motion of a VLFS was discussed. A remarkable mitigation of the heave motion of the platform due to the presence of the embedded OWC was found, particularly for longer incident waves.

ID 1383 track WDD
All authors are with the Department of Civil and Environmental Engineering of the University of Florence, Via di Santa Marta, 50139, Florence, Italy (e-mail: lorenzo.cappietti@unifi.it, irene.simonetti@unifi.it, ilaria.crema@unifi.it).

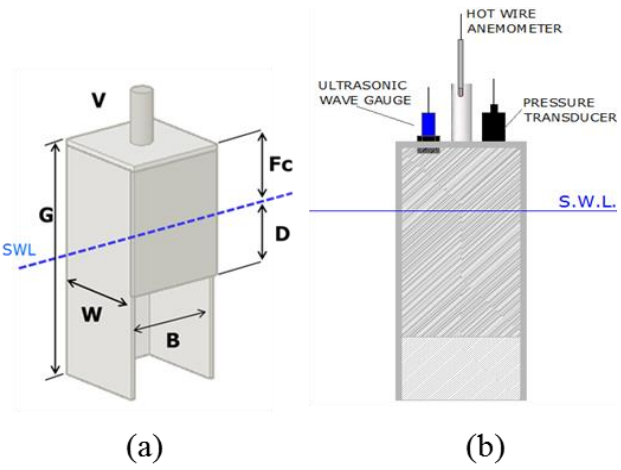

Fig. 1. Definition sketch of the OWC parameters (a) and experimental set-up (b).

This paper, specifically focusing on the wave energy conversion performance, is structured as follows: the laboratory test campaign performed on the fixed OWC and on the OWC integrated into the VLFS are introduced at first. Then, the hydrodynamic test conditions are presented and motivated, as well as the procedure for determining the OWC device performance. The differences of performance of the device in floating and fixed conditions on a set of test cases are finally shown.

II. LABORATORY-SCALE MODELLING

The experimental study was conducted at LABIMA, the Laboratory of Maritime Engineering (www.labima.unifi.it) of the Florence University.

The OWC laboratory-scale models were tested in a wave-current flume 37m long, 0.8m wide and high in 50cm of water depth. Each model comprises three adjacent OWC chambers that occupied almost the whole flume width. Each chamber had a rectangular cross-section with a circular vent on the top cover (Fig. 1), in order to introduce a quadratic air flow-pressure relation, which is typical for an impulse turbine (e.g. [4]).

Each OWC model was tested in fixed condition and floating condition. In the former case, each model was firmly connected to a fixed and rigid mounting system that suspended it 21cm above the bottom of the flume (measured form the lip of the back wall to the bottom of the flume), 22m from the wave maker.

In floating condition, each OWC was embodied in a laboratory-scale model of VLFS. The VLFS model was composed of several hollow building-blocks (BBs), open below the still water level and supported by an inner air-cushion. The concept of pressurized air-cushion systems has been already proposed in the literature for supporting semi-submersibles and concrete gravity structures, in order to stabilize the structure, reducing the VLFS displacements, drift forces and mooring loads [9-12].

To reproduce the dynamic similarity of the scale-model, considering the predominance of gravitational forces among those related to viscosity, the scale-models were

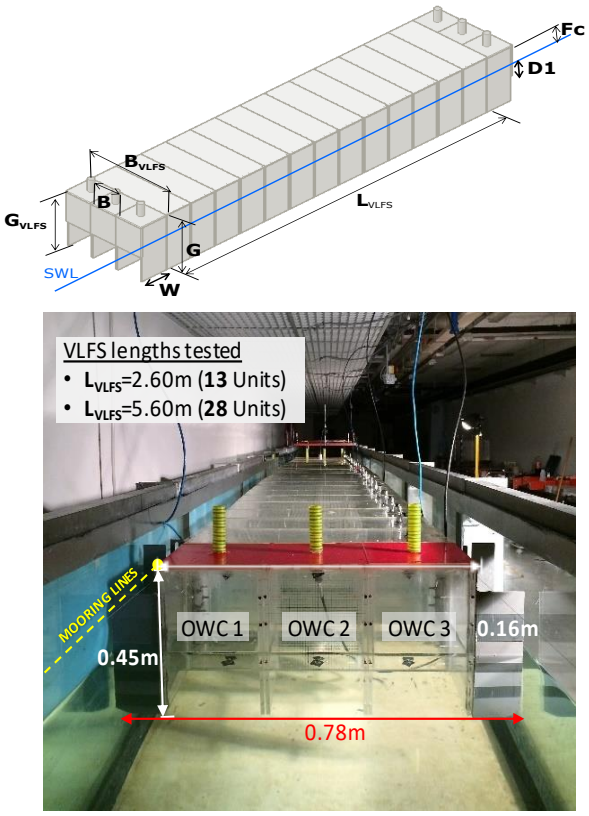

Fig. 2. Sketch of the VLFS laboratory-scale model embodying the OWC models at frontal and back edges.

designed according to Froude similarity, considering a 1:50 model scale.

It is well known [13-15] that the use of Froude similarity may lead to an improper scaling of the thermodynamic processes related to air compressibility in the OWC air chamber. Previous studies [15] pointed out that neglecting air compressibility when modelling the device at small scale may result in a moderate overestimation of the OWC capture width ratio (lower than 10% for the range of parameters of interest in this study). Since the aim of this study is the relative comparison among the performance of the device in fixed and floating (platform-embedded) conditions, the errors arising from neglecting air compressibility are considered negligible.

Another relevant aspect, which is worth to mention, is the scaling of air compressibility in the air-cushion system supporting the units of the VLFS in the laboratory model. At full scale, air-cushions may significantly modify the floating behaviour of the structure in waves, as studied e.g. in [16]. The compressibility of the air-cushion mainly depends on the height of the air chamber underneath the structure and, from a thermodynamic point of view, the process can be considered polytrophic. Due to the compressibility of air, the vertical restoring coefficient of an air-cushion supported structure is expected to be smaller than that of a conventional floater [16]. As for the air chamber of the OWC, applying an undistorted Froude scaling procedure to the air-cushion system may result in an improper reproduction of air compressibility effects, which should be further studied in a second stage of the the present work.

TABLE I
CODING AND DIMENSIONS OF THE TESTED OWC-VLFS GEOMETRIES

Chamber Thickness [cm]	
W1	**10**
W2	**20**
W3	**30**
Frontal wall draught [cm]	
D1	**7**
D2	18
D3	30
Top Cover Vent [% of the top cover area]	
V1	0.5
V2	**1.0**
V3	**2.0**
VLFS length [cm] / number of joined units (BB)	
L1	260 / 13 BB
L2	560 / 28 BB

In bold: OWC geometries tested in the platform-embodied conditions

A. Tested geometries and Laboratory set-up

Several OWC geometries were tested in order to perform a parametric study. The following design parameters were kept fixed (Fig. 1a):

- OWC chamber width orthogonal to the wave propagation direction: B=18.2cm,
- Freeboard: Fc=16cm above the still water level (SWL),
- Back wall height and side walls height: G=45cm.

The parameters varied during the physical tests were:

- the OWC chamber width along the wave propagation direction, W,
- the front wall draught, D,
- the diameter of the vent, V.

For the OWC in fixed conditions, three values for each parameter were tested for a total of 27 different OWC configurations (with values and coding as in Table I).

In floating platform-embodied conditions, OWC models with one value of the draught (D1), three widths (W1, W2 and W3) and 2 diameters of the vent (V2 and V3) were tested (Table I).

For the floating case, such OWC models were integrated as the frontal and back edges of the VLFS model (Fig. 2).

The building-blocks (BBs) of the VLFS were manufactured by using methacrylate panels (Fig. 2). Each BB is 0.60m wide, 0.45m high and 0.20m deep in direction of wave propagation. An air valve is installed on the roof of each unit, allowing to control its buoyancy by changing the pressure of the inner air cushion. The air pressure in the air-cushion support system of the VLFS units was settled in order to get the 16cm of freeboard above the SWL, as for the fixed OWC case.

Two VLFS models of different length where tested (Table I):

- a 2.6m long model, by assembling 13 BBs for a total weight of 980N,
- a 5.6m long model, by assembling 28 BBs, for a total weight of 2100N (Fig. 2).

The frontal edge of the VLFS models were placed 22m from the wave maker and were kept in position by means of four horizontal mooring lines to constrain it in surge and allow it to move in heave (two lines connected to the frontal edge and two to the back edge).

The mooring lines cables were made of 5m-long thin and high stiffness cotton rope. The mooring system was specifically conceived to reduce, practically to zero, the vertical mooring forces acting on the model during the tests, thus letting the structure to oscillate freely in heave.

Eleven ultrasonic distance sensors, characterized by a declared repeatability of 1mm, were deployed along the wave flume and the VLFS model.

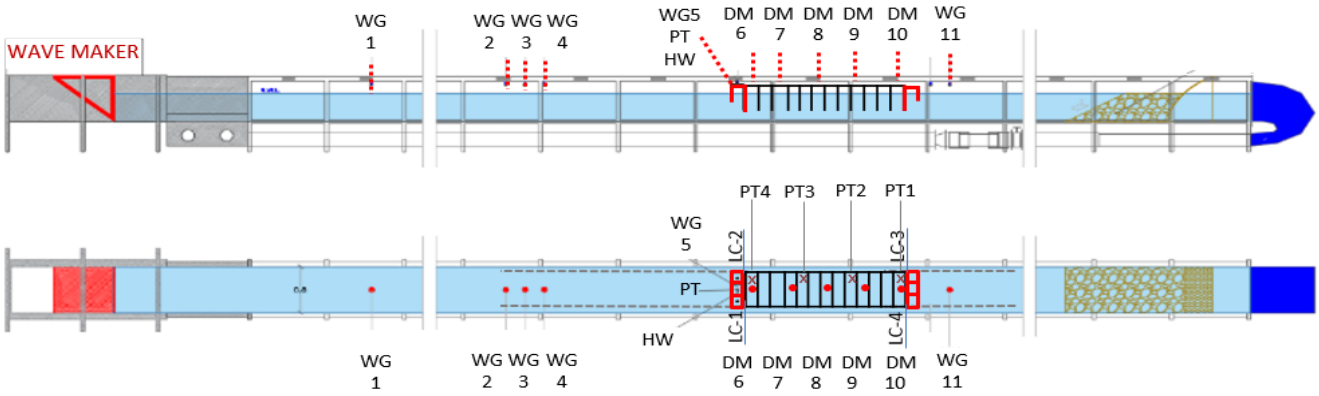

Fig. 3. Lay-out of the wave-flume, model setting and instrumentation.

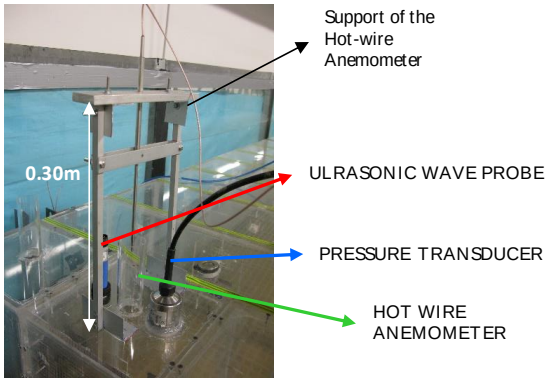

Fig. 4. Hot-wire anemometer, ultrasonic wave probe and pressure transducer equipping the top-cover pipe of the OWC model.

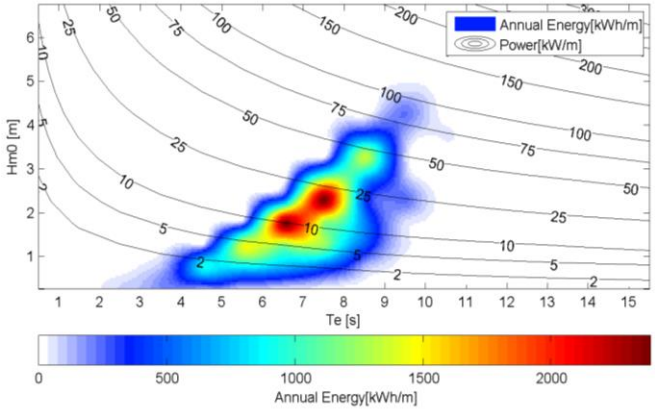

Fig. 5. Annual Energy for the Central Tuscany area (in terms of spectral wave height, H_{m0}, and energy wave period, T_e).

These sensors were used as wave gauges (WG) and as displacement meters (DM) to record the vertical motions of the VLFS model (Fig. 3):

- WG1, installed in front of the wave-maker for measuring the generated waves,
- WG2 to WG4, installed in front the models (OWC and OWC+VLFS) for measuring the incident and reflected waves,
- WG5, installed inside the OWC model at the VLFS frontal edge,
- DM6 to DM11 positioned above the VLFS model in order to measure its floating behaviour in heave,
- WG11 behind the model for measuring the transmitted waves.

Five pressure transducers (PT), with full scale range 100mbar and accuracy of ± 0.1% FS were installed in the VLFS model and in the OWC as follows:

- PT1-PT4, in the air cushion inside of the four units of the VLFS model, to register the air pressure variations during the tests,
- PT5, in the air pocket inside the OWC, to measure the internal pressure variations above the water free surface.

One Hot Wire (HW) anemometer, made of a platinum plated tungsten wire with a diameter of 5μm and a length of 1.25mm, was calibrated, ad hoc, in the interval range of 0-15m/s and was installed in the OWC vent, to measure the inlet and outlet airflow rate (Fig. 4).

III. HYDRODYNAMIC TEST CONDITIONS

The sea states simulated during the experimental tests (Table II) are representative of a hypothetical installation sea site located on a water depth of 25m, in front of the Tuscany coast, Italy (North Mediterranean Sea).

The assessment of the wave energy potential in the offshore of the Mediterranean Sea, as well as the site selection for possible installation of the OWC were previously conducted [17]. The results related to the Central Tuscany area are reprinted in Fig. 5. In terms of mean annual values, the selected site is characterized by a wave power of 2.8 kW/m. The sea states $1.0m \leq H_{m0} \leq 3.0m$ and $5.5s \leq T_e \leq 8.9s$ (where H_{m0} is the significant wave height and T_e is the energy period), having an occurrence frequency of 16%, are responsible of mean annual energy values above 1 MWh/m.

TABLE II
TESTED WAVE CONDITIONS (TARGET VALUES)

WAVE TYPE	WAVE CODE	H [cm]	T [s]
Regular	H01	4	0.8
Regular	H02	4	1.0
Regular	H03	4	1.4
WAVE TYPE	**WAVE CODE**	**H_{m0} [cm]**	**T_e [s]**
Irregular	H1	2	0.9
Irregular	H2	2	1.0
Irregular	H3	4	1.0
Irregular	H4	4	1.1
Irregular	H5	6	1.1

Overall, the wave conditions in Table II were tested and cover a range of wavelengths λ varying between 1 and 2.6m.

The longer VLFS tested has a length L2=5.6m, i.e. in the range $L2=5.6\text{-}2.15\lambda$. The VLFS with L2 can, therefore, be considered effectively as "very large", with reference to the wave climate of the reference installation site, according to the general definition of VLFS provided by [18].

IV. EXPERIMENTAL MEASUREMENTS

For the tested OWC and OWC+VLFS configurations, time-histories of incident wave, η_{inc}, OWC inner water surface oscillation, η, air velocity at the centre of the top cover pipe, U, and air pressure inside the OWC chamber, p(t), were measured at a sample frequency of 20 Hz. Fig. 6 shows examples of such time-history for one of the tested OWC configurations, for irregular incident waves.

A commonly used indicator of the performance of a WEC is the so-called Capture Width, CW [m], defined as the width of the wave front that contains the same amount of power as that absorbed by the device [19]. The capture width, CW [m] is therefore described as the ratio of the absorbed pneumatic power, Π_{OWC}, [W] to the wave power per unit length of the wave crest, Π_w, [W/m] (Eq.1):

$$CW = \frac{\overline{\Pi_{OWC}}}{\overline{\Pi_w}} \tag{1}$$

The absorbed pneumatic power is obtained through integration over the test duration T_{test} of the product of air pressure p, measured inside the OWC chamber, and airflow rate through the pipe, Q (Eq.2).

$$\overline{\Pi_{OWC}} = \frac{1}{T_{test}} \int_0^{T_{test}} Q(t)p(t)dt \tag{2}$$

For regular waves, the wave power per unit length of the wave crest is computed according to linear wave theory as in Eq. 3, where ρ is the water density, H is the regular wave height, ω is the wave frequency and k is the wave number, in given water depth h.

$$\overline{\Pi_{wave\ reg}} = \frac{1}{16}\rho g H^2 \frac{\omega}{k}\left(1 + \frac{2kh}{\sinh(2kh)}\right) \tag{3}$$

For irregular waves, the wave power is calculated as in Eq (4), where Si is the frequency spectrum, Δ_{fi} is the frequency resolution and $c_{g,i}$ is the wave group celerity of the spectral wave component of frequency f_i.

The group celerity is computed by solving the linear dispersion relation for the specific water depth h, and wave frequency f_i as in Eq. 5 in which, k_i is the wave number and ωi is the angular wave frequency.

$$\overline{\Pi_{wave\ irr}} = \rho g \sum_i c_{g,i} S_i \Delta f_i \tag{4}$$

$$c_{g,i} = \frac{1}{2}\left(1 + \frac{2k_i h}{\sinh(2k_i h)}\right)\frac{g}{\omega_i}\tanh(k_i h) \tag{5}$$

The capture width ratio, CW* [-], is then obtained as the ration between CW and the OWC chamber width, B, which for all the tests was fixed at 0.20m (Eq.6)

$$CW^* = CW/B \tag{6}$$

The results obtained for the performance of a floating OWC case W2D1V2, integrated in the VLFS of length L2=5.6m and tested under regular and irregular wave conditions, are reported in Table III. In regular waves, the maximum CW* for this OWC configuration is around 65% (for wave attack H02), obtained for the fixed condition. For the same wave, the VLFS-embodied conditions result in CW*=58%, i.e. around 10% lower.

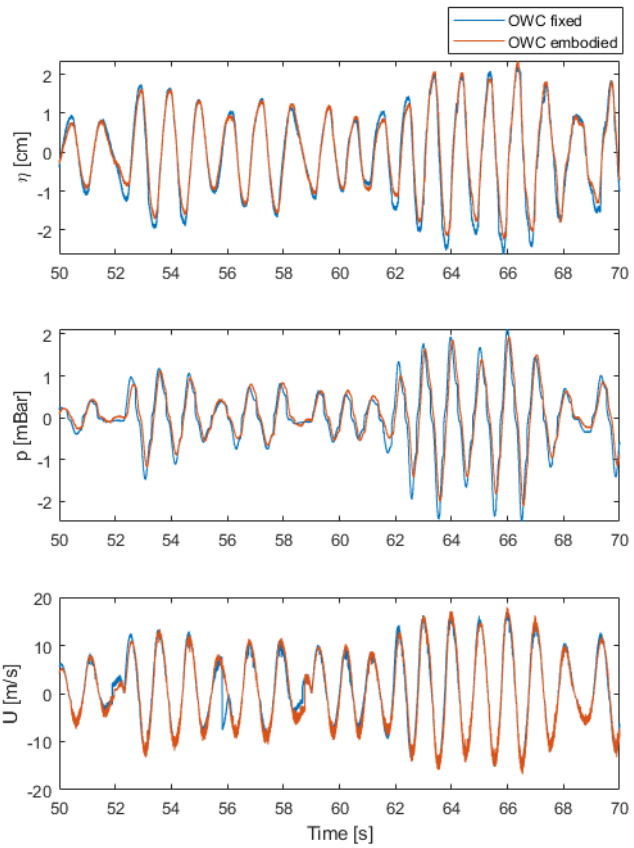

Fig.6. Time series of inner surface oscillation η, air chamber pressure p and air flow velocity in the vent centre U. Data are related to the OWC configuration W2D1V2 and the irregular incident wave H3.

TABLE III
CAPTURE WIDTH RATIO [%] OF THE OWC MODEL W2D1V2 IN FIXED & FLOATING CONDITIONS UNDER REGULAR AND IRREGULAR WAVES

WAVE TYPE	WAVE CODE	OWC in fixed Conditions	Floating Conditions VLFS length L2
Regular	H01	43	44
Regular	H02	65	58
Regular	H03	40	29
Irregular	H1	86	78
Irregular	H2	78	71
Irregular	H3	88	77
Irregular	H4	78	71
Irregular	H5	69	61

In the irregular wave cases (Tab. III, wave attacks H1 to H5) the pneumatic efficiency reaches a maximum value of about 88% for the fixed OWC device (obtained for the wave attack H3, H_{m0}=4cm and T_e=1s at laboratory scale 1:50). For the same wave attack, the OWC shows a slightly lower capture width ratio (77%, i.e. 12% lower) when it is embodied in the VLFS. It is worth to note that the OWC geometry W2D1V2 has a resonance frequency (estimated in the laboratory, by means of free decay tests documented in [6] and [20]) of around 1Hz (corresponding to an incident wave period of around 7s at full scale). All the tested irregular waves have periods

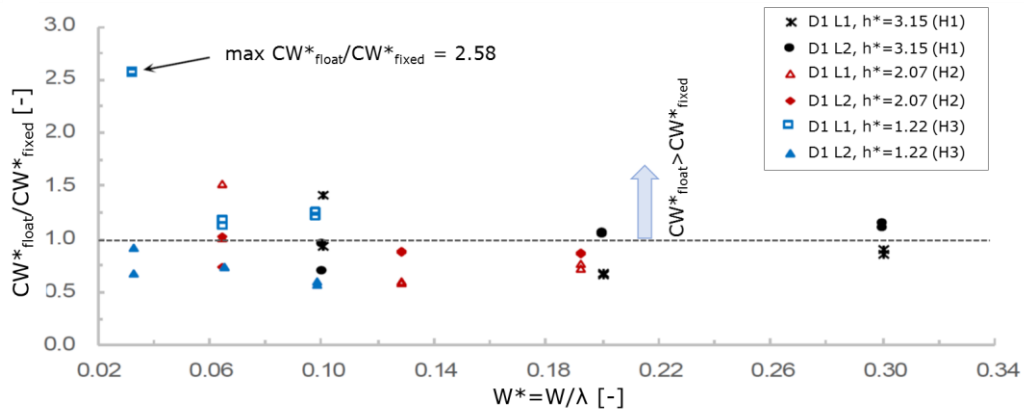

Fig. 7. Ratio of CW* for the floating OWC to that of the fixed OWC versus the relative width of the OWC chamber, W*=W/λ for different lengths of the VLFS (L1 and L2) and relative water depth h*=k·h. Results for regular waves.

TABLE IV
CAPTURE WIDTH RATIO [%] OF THE OWC MODEL W1D1V32 IN FIXED & FLOATING CONDITIONS UNDER REGULAR AND IRREGULAR WAVES

WAVE TYPE	WAVE CODE	OWC in Fixed Conditions	Floating Conditions VLFS length L2
Regular	H01	54	37
Regular	H02	48	35
Regular	H03	11	8
Irregular	H1	67	45
Irregular	H2	50	36
Irregular	H3	65	46
Irregular	H4	46	35
Irregular	H5	12	35

T_e close to that of resonance for the OWC, possibly explaining the higher values of CW* obtained in the irregular wave tests (as previously observed in [7]).

For the OWC+VLFS configuration W2D1V2-L2, the superposition of the motion of the VLFS (governed by elastic deformations) causes a moderate decrease of CW*, due e.g. to possible phase difference in the heave motion of the overall OWC+VLFS system and that of the inner water column of the OWC, resulting in a decrease of the relative free surface oscillation inside the device. For this specific case, it can be observed from the time series reported in Figure 6 that the embodied OWC exhibits both lower level of inner free surface oscillation and air pressure in the OWC chamber, resulting in a lower pneumatic efficiency.

The performance of the OWC case W1D1V3, fixed and integrated in the L2-VLFS, are reported in Table IV. This configuration is characterized by a smaller OWC chamber, associated to a lower applied damping. Overall, W1D1V3 geometry has lower CW* than W2D1V2, under all the tested wave attacks. The maximum CW* of the fixed OWC is around 54% in regular waves and 67% in irregular waves (for waves H01 and H1 respectively), coherently with the resonance frequency around 0.9Hz (T=6.4s at full scale) estimated for geometry W1D1V3; values of CW* up to 30% lowers are found in embodied conditions. A minimum CW* of 12% is found for the irregular wave attack H5, in fixed conditions. In this case, the superposition of the VLFS motion causes a relevant increase of CW* (almost 3 times), with CW*=35% for the platform-embodied conditions.

Overall, considering all the OWC-VLFS alternatives tested in regular waves (Figure 7), it can be observed that platform-embodied OWC may increase their CW* up to around 2.6 times, for specific OWC-VLFS configurations and wave conditions. In particular, higher CW* values in platform-embodied conditions are obtained mainly for relatively low values of the OWC chamber width compared to the incident wavelength (i.e., W*=W/λ<0.1). Increasing the value of the relative chamber width W*, CW* in floating and fixed conditions tends to have comparable values ($CW^*_{float}/CW^*_{fixed}$=~1).

An in-depth comparative analysis of the difference in the OWC performance in floating/fixed conditions and of the relation with the hydro-elastic motion of the VLFS under different incident waves is currently ongoing.

V. CONCLUDING REMARKS

In this work, the experimental campaign performed on a fixed OWC device and on the same OWC once embodied in a Very Large Floating Structure (VLFS) is presented.

The preliminary analysis of the results shows that the embodied OWC can have a higher wave energy conversion performance (expressed in terms of capture with ratio) than the corresponding fixed device for some specific geometry configuration and incident wave condition.

The integration of OWC device in VLFSs, which was previously proved to be a promising way of attenuating the motion of the VLFS (as discussed in [7]) may, therefore, be also beneficial to increase the overall harvested energy, enhancing the synergy of use of these two technologies.

An in-depth comparative analysis is ongoing, aimed at discussing the effect of different design parameters of the OWC (draught, width, damping applied by the turbine), of the VLFS length and of the incident wave conditions

(period, height) on both the motion of the VLFS and the wave energy conversion performance of the OWC.

Moreover, the effect of applying Froude similarity for scaling the air-cushion system of the VLFS model (and the related implications of air compressibility on the overall dynamics of the system) should be further studied as future extensions of the present work.

ACKNOWLEDGEMENT

The support of Civil and Environmental Engineering Department of Florence University under the NEMO project and the EU-H2020 MARINET2 project under the LABIMA-UNIFI partner are gratefully acknowledged.

REFERENCES

[1] A.F. de O. Falcão, "Wave energy utilization: A review of the technologies", *Renewable and Sustainable Energy Reviews*, vol. 14, pp: 899-918. 2010.

[2] C.B. Boake, T.J.T. Whittaker, M. Folley, H. Ellen, "Overview and Initial Operational Experience of the LIMPET Wave Energy Plant", *12th Int. Offshore Polar Eng. Conf.* 2002.

[3] Y. Torre-Enciso, I. Ortubia, L.I.L De Aguileta, J. Marqués. "Mutriku Wave Power Plant: from the thinking out to the reality", *8th Eur. Wave Tidal Energy Conf.*, 2009.

[4] A.F. de O. Falcão, L.M.C. Gato, E.P.A.S Nunes, "A novel radial self-rectifying air turbine for use in wave energy converters. Part 2. Results from model testing", *Renewable Energy*, vol. 3, pp: 159-164. 2013.

[5] C.M. Wang, Z.Y. Tay, K. Takagi, T. Utsunomiya, "Literature Review of Methods for Mitigating Hydroelastic Response of VLFS Under Wave Action." *Applied Mechanics Reviews*, vol. 63(3), p. 18. 2010.

[6] I. Crema, I. Simonetti, L. Cappietti, H. Oumeraci, "Laboratory Experiments on Oscillating Water Column Wave Energy Converters Integrated in a Very Large Floating structure", *11th Eur. Wave and Tidal Energy Conf*. 2015.

[7] I. Crema, L. Cappietti, "Experimental Modelling of Very Large Floating Structures Equipped with OWC type WECs: harvesting of the energy and damping effects", *8th Int. Short Course/Conf. on Applied Coastal Research*. 2017.

[8] I. Simonetti, L Cappietti, H. ElSafti, H. Oumeraci "Optimization of the geometry and the turbine induced damping for fixed detached and asymmetric OWC devices: A numerical study", *Energy*, vol. 139, pp: 1197-1209. 2017.

[9] J.A. Pinkster, A. Fauzi, Y. Inoue, S. Tabeta. "The behavior of large air cushion supported structures in waves." *Hydroelasticity in Marine Technology*, pp. 497-506. 1998.

[10] T. Ikoma, K. Masuda, C.-K. Rheem, H. Maeda, R. Iwasa. "Hydroelastic behavior of air-supported flexible floating structures", *23rd Int. Conf. on Offshore Mechanics and Arctic Eng.* 2004.

[11] K.P.T. Thiagarajan, M. Morris-Thomas, "Wave-induced Motions of an Air Cushion in Shallow Water", *Ocean Eng*, vol. 33, pp. 143–1160. 2006.

[12] J.A. Pinkster, E.J.A. Meevers Scholte, "The behavior of a large air-supported MOB at sea", *Marine Structures*, vol. 14, pp. 163-179, 2001.

[13] A.F. de O. Falcão, J.C.C. Henriques, "Model-prototype similarity of oscillating water-column wave energy converters", *Int. J. Mar. Energy*, 6, 18-34. 2014.

[14] W. Sheng, R. Alcorn, A. Lewis. "On thermodynamics in the primary power conversion of oscillating water column wave energy converters", *J. Renew. Sustain. Energy*, vol. 5 (2). 2014.

[15] I. Simonetti, L. Cappietti, H. ElSfati, H., Oumeraci, "Evaluation of air compressibility effects on the performance of fixed OWC wave energy converters using CFD modelling", *Renewable Energy*, vol. 119, pp. 741-753. 2017.

[16] J.L.F van Kessel, "Aircushion Supported Mega-Floaters", Delft University of Technology & SBM Gusto. 2010.

[17] V. Vannucchi, L. Cappietti, "Wave energy estimation in four Italian Nearshore Areas", *32nd International Conference on Ocean, Offshore and Arctic Engineering*, 2013.

[18] H. Suzuki, K. Yoshida, "Design flow and strategy for safety of very large floating structures", *Int. workshop on very large floating structures*, pp. 21–27. 1996.

[19] A. Price, C.J. Dent, A.R. Wallace, "On the capture width of wave energy converters", *Applied Ocean Research*, vol. 31(4), pp: 251-259. 2009.

[20] I. Crema, "Oscillating Water Column wave energy converters integrated in Very Large Floating Structures". PhD thesis. *University of Florence & University of Braunschweig – Institute of Technology*. 2018.